Evaluation of Chlorophyll-Related Vegetation Indices Using Simulated Sentinel-2 Data for Estimation of Crop Fraction of Absorbed Photosynthetically Active Radiation

Taifeng Dong, Jihua Meng, Jiali Shang, *Member, IEEE*, Jiangui Liu, and Bingfang Wu

***Abstract*—In recent years, the impact of chlorophyll content on the estimation of the fraction of absorbed photosynthetically active radiation (FPAR) has attracted increased attention. In this study, chlorophyll-related vegetation indices (VIs) were selected and tested for their capability in crop FPAR estimation using simulated Sentinel-2 data. These indices can be categorized into four classes: 1) the ratio indices; 2) the normalized difference indices; 3) the triangular area-based indices; and 4) the integrated indices. Two crops, wheat and corn, with distinctive canopy and leaf structure were studied. Measured FPAR and Sentinel-2 reflectance simulated from field spectral measurements were used. The results showed that VIs using the near-infrared and red-edge reflectance, including the modified Simple Ratio-2 (mSR2), the red-edge Simple Ratio (SR_{705}), the Red-Edge Normalized Difference Vegetation Index (ND_{705}), MERIS Terrestrial Chlorophyll Index (MTCI), and the Revised Optimized Soil-Adjusted Vegetation Index (OSAVI[705, 750]), had a strong linear correlation with FPAR, especially in the high biomass range. When the red-edge reflectance was used, the ratio indices (e.g., mSR2 and SR_{705}) had a stronger correlation with crop FPAR than the normalized difference indices (e.g., ND_{705}). Sensitivity analysis showed that mSR2 had the strongest linear correlation with FPAR of the two crops across a growing season. Further analysis indicated that indices using the red-edge reflectance might be useful for developing FPAR retrieval algorithms that are independent of crop types. This suggests the potential for high resolution and high-quality mapping of FPAR for precision farming using the Sentinel-2 data.**

Manuscript received July 07, 2014; revised January 03, 2015; accepted January 28, 2015. Date of publication February 25, 2015; date of current version September 12, 2015. This work was supported in part by the "Strategic Priority Research Program-Climate Change: Carbon Budget and Related Issues" of the Chinese Academy of Science under Grant XDA05050109, in part by the National High Technology Research and Development Program of China (863 program) under Grant 2012AA12A307, in part by the International Science and Technology Cooperation Program of China under Grant 2011DFG72280, and in part by the China Grains Administration Special Fund for Public Interest under Grant 201313009-02. *(Corresponding author: Bingfang Wu.)*

T. Dong is with the Division for Digital Agriculture, Key Laboratory of Digital Earth Science, Institute of Remote Sensing and Digital Earth, Chinese Academy of Sciences, Beijing 100101, China, and also with the Eastern Cereal and Oilseed Research Centre, Agriculture and Agri-Food Canada, Ottawa, ON K1A0C6, Canada (e-mail: dong.taifeng@gmail.com).

J. Meng and B. Wu are with the Division for Digital Agriculture, Key Laboratory of Digital Earth Science, Institute of Remote Sensing and Digital Earth, Chinese Academy of Sciences, Beijing 100101, China (e-mail: mengjh@radi.ac.cn; wubf@radi.ac.cn).

J. Shang and J. Liu are with the Eastern Cereal and Oilseed Research Centre, Agriculture and Agri-Food Canada, Ottawa, ON K1A0C6, Canada (e-mail: Jiali.Shang@AGR.GC.CA; Jiangui.Liu@AGR.GC.CA).

Digital Object Identifier 10.1109/JSTARS.2015.2400134

***Index Terms*—Chlorophyll-related vegetation indices, crop FPAR, red-edge reflectance, Sentinel-2.**

I. Introduction

THE FRACTION of absorbed photosynthetically active radiation (FPAR), defined as the fraction of photosynthetically active radiation (PAR) absorbed by vegetation canopy in the 0.4–0.7 μm spectrum range [1], [2], is a critical biophysical parameter for assessing vegetation growth rate and predicting crop productivity [1], [3]–[5]. It is also an essential climate variable (ECV) used for assessing carbon budget under climate change [6]. Therefore, accurate estimation of FPAR is critical for improving vegetation growth modeling [7], [8].

Due to their time and spatial continuity, satellite remote sensing data have been widely used for FPAR estimation [4], [9]–[15]. A great number of studies have shown that FPAR can be successfully retrieved either from vegetation indices (VIs) using a statistical model [5], [6], [12], [16], [17] or from the inversion of a canopy reflectance model [9], [11], [13], [14], [18]–[20]. Methods using VIs are used more often than that based on canopy reflectance model inversion. Most of the VIs are mathematical functions of the visible and near-infrared reflectance (NIR) that can effectively reveal canopy photosynthetic capacity. The visible reflectance captures the greenness (e.g., chlorophyll content) while the NIR captures canopy structural properties [e.g., LAI and leaf angle distribution (LAD)] [16], [17], [21]–[23]. Thus, VIs could be used as a surrogate of FPAR [15], [23], [24]. The Normalized Difference Vegetation Index (NDVI) is the most widely used VI for FPAR estimation across different vegetation types [5], [12], [16], [17], [19], [22]; however, it tends to lose sensitivity to FPAR when FPAR is greater than 0.7 [23]. One reason is that the red reflectance becomes insensitive to variation in canopy chlorophyll content at moderate-to-high leaf area index (LAI). In recent years, other indices have been developed or tested for FPAR estimation. These include the Renormalized Difference Vegetation Index (RDVI) combining the advantages of NDVI and the Difference Vegetation Index (DVI) [12], the Enhanced Vegetation Index (EVI) integrating the blue reflectance to correct for aerosol effect [10], the Green NDVI replacing the red reflectance with the green reflectance in NDVI [15], the second Modified Triangular Vegetation Index (MTVI2) incorporating a soil

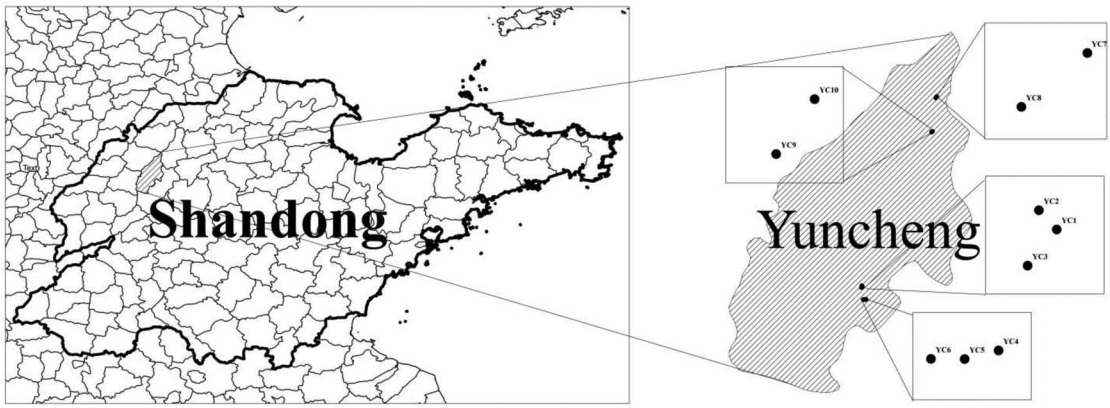

Fig. 1. Study site in Yucheng, Shangdong Province, China.

adjustment factor [12], the Red-edge NDVI replacing the red reflectance with the red-edge reflectance in NDVI [25], and the Wide Dynamic Range Vegetation Index (WDRVI) integrating a weighting coefficient in NDVI to enhance the sensitivity of NIR reflectance to biophysical variables at moderate-to-high vegetation density [12]. Compared with NDVI, these VIs show stronger correlations with FPAR and are more sensitive to FPAR when LAI is large [10], [12].

FPAR is generally considered as a function of canopy structural properties (e.g., LAI and LAD) [25]. Recent studies indicate that only the portion of PAR absorbed by the photosynthetic components of a canopy is directly related to photosynthesis and biomass production [26], [27]. To improve the estimation accuracy of FPAR for terrestrial carbon assimilation studies, the proportion due to non-photosynthetic components should be excluded [27]–[30]. Chlorophyll is the most important pigment in the green tissues for photosynthesis and biomass production [30]–[32]. Studies show that the contribution of leaf chlorophyll concentration to FPAR variability is negligible at the early vegetative growth stages, but becomes dominant starting from the exuberant growth periods [33]. Studies by Zhang and coworkers [4], [8], [29] showed that FPAR could be reliably approximated by the EVI because EVI had a better capability to capture canopy greenness and to correct for influences from variability of canopy background reflectance and atmospheric conditions. The studies by Gitelson and Gamon [27] showed that the increase in crop FPAR, especially the portion corresponding to the green plant components ($\mathrm{FPAR}_{\mathrm{green}}$), coincided with the increase in canopy chlorophyll content during the vegetative growth stages for both corn and soybean. Peng *et al.* [32] observed that $\mathrm{FPAR}_{\mathrm{green}}$ has a good correlation with total chlorophyll content in corn. Some chlorophyll-related VIs, such as the MERIS Terrestrial Chlorophyll Index (MTCI) [34], the red-edge NDVI [12], the Green Chlorophyll Index ($\mathrm{CI}_{\mathrm{green}}$) [32], the Red-Edge Chlorophyll Index ($\mathrm{CI}_{\mathrm{red\text{-}edge}}$) [32], and the WDRVI [12], [32] are proven to be more sensitive to FPAR at high LAI. Studies demonstrate that in addition to LAI, leaf chlorophyll content is another important factor influencing the variation in FPAR [12], [31]–[33]. Thus, it can be concluded that canopy chlorophyll content is closely correlated with $\mathrm{FPAR}_{\mathrm{green}}$ [32], [35].

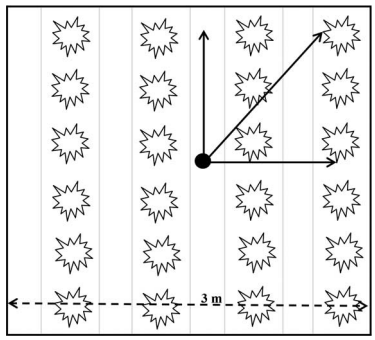

Fig. 2. Illustration of FPAR measurement.

More recently, many chlorophyll-related VIs, especially the indices based on the red-edge reflectance, have been successfully used for leaf or canopy chlorophyll content estimation [32], [36]–[41]. For examples, the ratio of the Transformed Chlorophyll Absorption in Reflectance Index to the Optimized Soil-Adjusted Vegetation Index (TCARI/OSAVI) [40] and the ratio of the Modified Chlorophyll Absorption Ratio Index (MCARI) to the OSAVI (MCARI/OSAVI) [42] have been found to be sensitive to leaf chlorophyll content. Wu *et al.* [37] found that when the red reflectance at 670 nm was replaced by the red-edge reflectance at 705 nm and the reflectance at 700 nm was replaced by the red-edge reflectance at 750 nm, the above two combinations of indices can be used for canopy chlorophyll content estimation. This is because the red-edge reflectance is sensitive to both leaf chlorophyll content and LAI [43], [44]. The $\mathrm{CI}_{\mathrm{green}}$ and the $\mathrm{CI}_{\mathrm{red\text{-}edge}}$ were found to improve the accuracy of canopy chlorophyll content estimation significantly [39], [45], [46], and the MTCI incorporating the red-edge reflectance provided a robust canopy chlorophyll content estimation across different crops [47], [48].

The abilities of the above indices for FPAR estimation have been explored in several studies [34], [48], [49]. Mostly these studies have focused on a single crop type, and no comprehensive analysis has been made on comparison of the indices for FPAR estimation on different crops. The red-edge indices are proven to be advantageous for LAI or chlorophyll content estimation over different crop types [43], [49], [50], but no study has attempted to evaluate their performance for FPAR

TABLE I
CHLOROPHYLL-RELATED VIs SELECTED IN THIS STUDY

Name	Index	Formulation	Scale	References	Bands used
		Normalized difference indices			
Normalized Difference Vegetation Index	NDVI	$(R_{800}-R_{670})/(R_{800}+R_{670})$	Canopy	[54]	783, 665
Normalized Difference Red-edge Index	ND_{705}	$(R_{750}-R_{705})/(R_{750}+R_{705})$	Canopy	[55], [56]	740, 705
MERIS terrestrial chlorophyll index	MTCI	$(R_{750}-R_{710})/(R_{710}-R_{680})$	Canopy	[47]	750, 705, 665
Renormalized Difference Vegetation Index	RDVI	$(R_{800}-R_{670})/\sqrt{R_{800}+R_{670}}$	Canopy	[38]	783, 665
Renormalized Difference Vegetation Index[800,705]	$RDVI_{705}$	$(R_{800}-R_{705})/\sqrt{R_{800}+R_{705}}$	Canopy	[57]	783, 705
Green NDVI	GNDVI	$(R_{800}-R_{550})/(R_{800}+R_{550})$	Canopy	[58]	783, 560
mNDVI	mNDVI	$(R_{800}-R_{680})/(R_{800}+R_{680}-2R_{445})$	Canopy	[56]	783, 665, 443
mNDVI[705,750]	mND_{705}	$(R_{750}-R_{705})/(R_{750}+R_{705}-2R_{445})$	Canopy	[56]	740, 705, 443
Optimized Soil-Adjusted Vegetation Index	OSAVI	$(R_{800}-R_{670})/(R_{800}+R_{670}+0.16)$	Canopy	[59]	783, 665
OSAVI[705,750]	OSAVI[705,750]	$(R_{750}-R_{705})/(R_{750}+R_{705}+0.16)$	Canopy	[37]	740, 705
		Ratio indices			
Modified Simple Ratio	mSR	$(R_{800}/R_{670}-1)/\sqrt{R_{800}/R_{670}+1}$	Canopy	[60]	783, 665
mSR[705,750]	mSR2	$(R_{750}/R_{705}-1)/\sqrt{R_{750}/R_{705}+1}$	Canopy	[37]	740, 705
Simple Ratio	SR	R_{800}/R_{670}	Canopy	[61]	783, 665
SR[705,750]	SR_{705}	R_{750}/R_{705}	Canopy	[55], [56]	740, 705
Red-edge Chlorophyll index	$CI_{red\text{-}edge}$[705]	$R_{800}/R_{705}-1$	Canopy	[39], [44]	783, 705
$CI_{red\text{-}edge}$[750]	$CI_{red\text{-}edge}$[750]	$R_{800}/R_{750}-1$	Canopy	[39], [44]	783, 740
Green Chlorophyll index	CI_{green}	$R_{800}/R_{550}-1$	Canopy	[39]	740, 560
		Triangular area based indices			
Triangular Vegetation Index	TVI	$0.5(120(R_{800}-R_{550})-200(R_{670}-R_{550}))$	canopy	[62]	783, 665, 560
Triangular Greenness Index	TGI	$-0.5((\lambda_r-\lambda_b)(R_r-R_g)-(\lambda_r-\lambda_g)(R_r-R_b))$	Leaf	[63]	665, 560, 490
		Integrated indices			
Triangular Chlorophyll Index	TCI	$1.2(R_{700}-R_{550})-1.5(R_{670}-R_{550})\sqrt{R_{700}/R_{670}}$	Leaf	[38]	705, 665, 560
Modified Chlorophyll Absorption Ratio Index	MCARI	$((R_{700}-R_{670})-0.2(R_{700}-R_{550}))(R_{700}/R_{670})$	Leaf	[40]	705, 665, 560
MCARI[705,750]	MCARI[705,750]	$((R_{750}-R_{705})-0.2(R_{750}-R_{550}))(R_{750}/R_{705})$	Canopy	[37]	740, 705, 560
Transformed Chlorophyll Absorption Ratio Index	TCARI	$3*((R_{700}-R_{670})-0.2(R_{700}-R_{550})(R_{700}/R_{670}))$	Leaf	[40]	705, 665, 560
TCARI[705,750]	TCARI[705,750]	$((R_{750}-R_{705})-0.2(R_{750}-R_{550})(R_{750}/R_{705}))$	Canopy	[37]	740, 705, 560
TCARI/OSAVI	TCARI/OSAVI	TCARI/OSAVI	Leaf	[40], [64]	783, 705, 665, 560
TCARI/OSAVI[705,750]	TCARI/OSAVI[705,750]	TCARI[705,750]/ROSAVI[705,750]	Canopy	[37]	740, 705, 560
MCARI/OSAVI	MCARI/OSAVI	MCARI/OSAVI	leaf	[40]	783, 705, 665, 560
MCARI/OSAVI[705,750]	MCARI/OSAVI[705,750]	MCARI[705,750]/OSAVI[705,750]	Canopy	[37]	740, 705, 560

estimation. To assess the abilities of these indices for the estimation of crop FPAR, two common crops with significantly different crop structures were selected: 1) the wheat from C3 plants and 2) the corn from C4 plants. Since FPAR is nearly equal to $\mathrm{FPAR}_{\mathrm{green}}$ during the vegetative growth stages [5], [12], [43], we restricted our study only to these development stages. The objectives are 1) to compare the performance of different chlorophyll-related VIs for FPAR estimation and 2) to evaluate the use of red-edge reflectance in the estimation of FPAR of different crops. A regression and sensitivity analysis approach was used in the study.

II. DATA AND METHODS

A. Site Description

The experiments were carried out at the Yucheng study site ($36^\circ 50'\mathrm{N}$, $116^\circ 33'\mathrm{E}$) in Shandon province, China (Fig. 1). It is located in the North China Plain, within the temperate semi-arid monsoon climate zone with a cold winter and a hot summer. The annual mean temperature and precipitation were $13.3^\circ\mathrm{C}$ and 555.5 mm, respectively. Its long frost-free period, about 202 days per year, is ideal for the winter wheat-corn cropping rotation. The winter wheat is usually seeded in early October

of the previous year. Its growing period is from March to early June and harvest is in early to mid-June. Corn is seeded immediately afterward and the growing period is between late June and October.

B. Experimental Design

The experiments were conducted on two crops, 1) winter wheat and 2) corn, during the 2012 growing season. Four fields with typical winter wheat-corn rotation were selected. A total of 10 plots with an area of 60 m by 60 m each were deployed inside the four fields (Fig. 1). For each large plot, five smaller plots of 3 m $\times$ 3 m were randomly deployed along the diagonal for intensive field measurements. For the winter wheat, data collections were carried out during three periods: 1) March 25th to 28th (the jointing stage); 2) April 16th to 19th (the booting stage); and 3) May 10th to 14th (the flowering stage). For the corn, data collections were also conducted during three periods: 1) July 12th to 15th (the V3 or the third leaf collar stage); 2) August 16th to 19th (the V7 or the seven leaf collar stage); and 3) in early September when corn was at tassel emergence stage (the VT stage).

Field data including canopy reflectance and FPAR was made on clear sky conditions and close to local solar noon (between 10:30 and 13:00 local time) to minimize the effects of variation in solar zenith angle. Measurements made with a solar zenith angle (SZA) larger than 45° were excluded, leaving a total of 187 samples, 104 for corn and 83 for wheat.

C. FPAR Measurements

The SUNSCAN Canopy Analysis system (Delta-T Devices, Cambridge, UK) was used for FPAR measurements. The SUNSCAN includes a 1-m probe and a handheld PDA. A total of 64 quantum sensors are embedded in the probe, and an RS-232 cable is used to connect the probe and the PDA. The output unit of each sensor was measured in $\mathrm{mol\ m^{-2}\ s^{-1}}$. For each measurement, the average of the readings from the 64 sensors is transmitted to and stored in the PDA. FPAR is derived from four PAR measurements according to the following equation [12]:

$$FPAR = ((PAR_0 - PAR_{\mathrm{c}}) - (PAR_t - PAR_{\mathrm{g}}))/PAR_0. \quad (1)$$

where PAR_0 is the incident PAR measured using the SUNSCAN at about 1 m above the canopy with the sensors facing the sky; PAR_{c} is PAR reflected from the canopy, measured with the sensors facing the canopy downward from the same height as measuring PAR_0; PAR_{t} is the PAR transmitted through a canopy and measured with the SUNSCAN facing upward at about 2 cm above the ground; PAR_{g} is reflected PAR from the soil, and measured with the SUNSCAN facing downward at the same height as measuring PAR_{t}. The purpose of measuring PAR_{t} and PAR_{g} is to eliminate the portion of PAR absorbed by the ground (e.g., soil). At each small plot, three sets of PAR measurements (a total of 12 PAR readings) were taken with the probe oriented along the row, perpendicular to the row and at a 45° angle with the row directions (Fig. 2). The average of the three FPAR derived from the three sets of measurements was used as the FPAR of a small plot.

TABLE II
RESULTS OF THE LINEAR REGRESSION BETWEEN FPAR AND VIS, WITH THE SAMPLES FROM BOTH THE WHEAT AND CORN

Vegetation index	Regression model	R^2	RMSE
mSR2	y = 0.512x+0.002	0.89*	0.09
SR_{705}	y = 0.186x+0.107	0.87*	0.10
ND_{705}	y = 1.427x–0.154	0.87*	0.10
mSR	y = 0.170x+0.093	0.87*	0.10
MTCI	y = 0.053x+0.110	0.86*	0.10
OSAVI[705,750]	y = 2.169x–0.167	0.85*	0.11
NDVI	y = 1.216x–0.346	0.85*	0.11
TCARI/OSAVI[705,750]	y = –0.629x+0.765	0.83*	0.11
GNDVI	y = 1.691x–0.485	0.83*	0.11
RDVI705	y = 1.807x–0.124	0.83*	0.11
$CI_{\text{red-edge}}$[750]	y = 0.104x+0.165	0.83*	0.11
mND_{705}	y = 1.354x–0.248	0.82*	0.12
RDVI	y = 1.758x–0.252	0.81*	0.12
MCARI/OSAVI[705,750]	y = 0.456x–0.037	0.81*	0.12
MCARI[705,750]	y = 0.777x+0.173	0.80*	0.12
$CI_{\text{red-edge}}$[705]	y = 1.517x+0.073	0.78*	0.13
CI_{green}	y = 0.069x+0.153	0.78*	0.13
mNDVI	y = 1.304x–0.588	0.76*	0.13
OSAVI	y = 3.895x–0.167	0.74*	0.14
SR	y = 0.025x+0.257	0.74*	0.14
TVI	y = 0.035x–0.077	0.70*	0.15
TCARI/OSAVI	y = –0.831x+0.973	0.59*	0.17
TCARI[705,750]	y = –1.800x+0.651	0.46*	0.20
MCARI	y = 4.831x+0.137	0.41*	0.21
TCI	y = 6.001x+0.110	0.23*	0.23
TCARI	y = –1.152x+0.581	0.01	0.27
TGI	y = –0.031x+0.545	0.01	0.27
MCARI/OSAVI	y = 0.011x+0.475	0.00	0.27

Note: x represents VI and y represents FPAR; R^2 is the coefficient of determination; RMSE is the RMSE of FPAR; * refers to a significant correlation at 0.01 level; total number of samples = 187.

There are limitations for satellite-based and field-measured FPAR, as they provide instantaneous FPAR estimation, whereas vegetation productivity models, particularly the light use efficiency model, require daily integrated FPAR including direct and diffused FPAR [3]–[6], [12]. Studies indicate that the instantaneous black-sky FPAR at solar noon is approximate to the daily black-sky-integrated FPAR [24], [51]. For assessing the relationships between VIs and FPAR without considering the effect of illumination conditions, our FPAR measurements were limited to a time period during the solar noon (10:30 to 13:00) under clean sky. As all the FPAR measurements were conducted before the reproductive stage of the crops, the obtained FPAR was considered to be equal to $\mathrm{FPAR}_{\mathrm{green}}$ in this study.

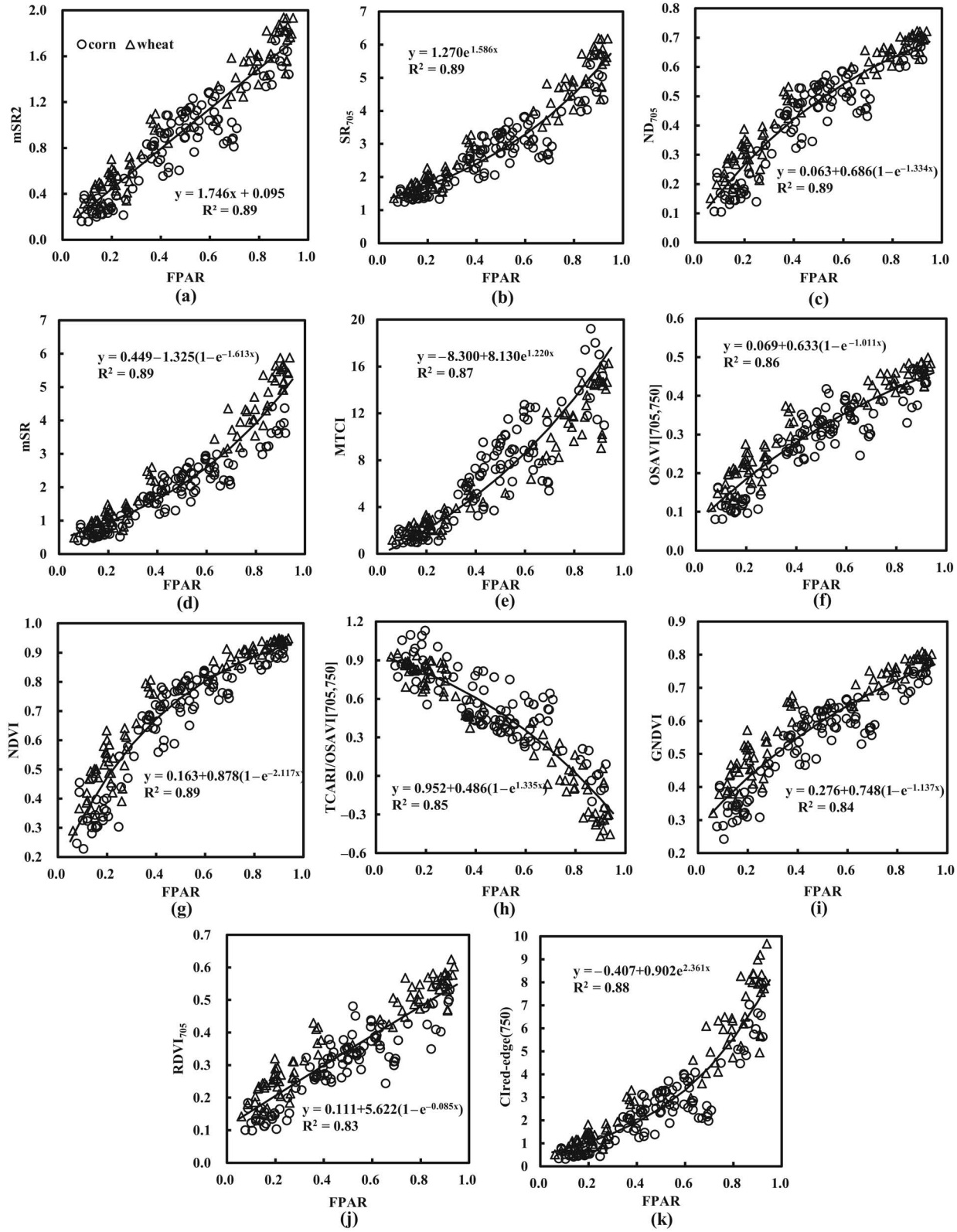

Fig. 3. Relationship between FPAR and VIs with a linear R^2 larger than 0.83.

D. Canopy Spectral Reflectance Measurement and VI Calculation

Canopy spectral reflectance was measured using the portable field spectroradiometer HR-786 [Spectra Vista Corporation (SVC), Poughkeepsie, NY, USA]. The spectral range covers from 350 to 2500 nm, with a resolution of 1.5 nm from 350 to 1000 nm, 7.5 nm from 1000 to 1850 nm, and 5 nm from 1850 to 2500 nm. Measurements were taken with a fiber optics

of 25° field of view (FOV) under a clear and stable air condition. Spectral radiance of crop canopy was measured with the fiber optics pointing downward at 1.5 m above the canopy, and that of a barium sulfate ($BaSO_4$) was measured under the same illumination condition as reference to convert canopy spectral radiance to reflectance. For each plot, a reference measurement was made first, followed by five target measurements to obtain an average spectrum for the plot.

In this study, 28 chlorophyll-related VIs were selected and evaluated for FPAR estimation. These indices, with their names, formula, and references, are listed in Table I. The selected VIs can be classified into four classes, namely, 1) the normalized difference indices; 2) the ratio indices; 3) the triangular area-based indices; and 4) the integrated indices combining two VIs. The reflectance spectra were smoothed first using the Savitzky–Golay filtering method [52] to reduce noise. The derived spectra were then resampled to the seven bands corresponding to that of the Sentinel-2 satellite sensor, with center wavelength at 443, 490, 560, 665, 705, 740, and 783 nm (bands 1–7). The resampling was made using the spectral response function found in Segl *et al.* for the Sentinel-2 sensor [53]

$$R_K(\lambda) = \chi_0 + \chi_s * e^{-|2(\lambda-\lambda_c)/\alpha\Delta\lambda|^{X_e}} \quad (2)$$

where k is the band number, $\Delta\lambda$ is the full-width-half-maximum (FWHM) of the spectral filter functions, and λ_c is the center wavelength; parameters X_e equals to 6, X_0 equals to 0.0001, X_s equals to 0.8999, and α equals to 1.06299.

E. Regression Analysis and Sensitivity Study

Ideally, the best VI for crop FPAR estimation should be linearly correlated with crop FPAR [24]. Thus, a linear regression analysis between the measured FPAR and the derived VIs was performed first to select VIs for further analyses. The coefficient of determination (R^2) and the root-mean-square error (RMSE) were employed as metrics for the selection. In the second step, further analyses were made to evaluate the indices selected from the initial linear regression analysis, for their abilities in FPAR estimation across the two crops.

The best-fit linear or nonlinear regression models were built using the samples of each individual crop (crop specific models), and using the samples of the two crops combined (the combined model). RMSE of FPAR estimation was calculated for each of the regression models and sample sets, and the following indicators were derived to characterize the performance of an index:

$$\begin{aligned} R_C &= 100 \times |(RMSE_{\mathrm{IC}} - RMSE_{\mathrm{TC}})|/RMSE_{\mathrm{TC}} \\ R_W &= 100 \times |(RMSE_{\mathrm{IW}} - RMSE_{\mathrm{TW}})|/RMSE_{\mathrm{TW}} \\ R_T &= 100 \times |(RMSE_{\mathrm{IT}} - RMSE_{\mathrm{TT}})|/RMSE_{\mathrm{TT}} \end{aligned} \quad (3)$$

where R_C, R_W, and R_T represent percentage variation in estimation errors between the errors obtained using the crop specific regression models and that obtained using the combined regression model for corn, wheat, and the two crops combined, respectively. RMSE to the right of the equation represent RMSE of FPAR derived for a certain sample set (represented by the second subscript letter, with C, W, and T represent sample sets of corn, wheat, and the two crops combined) using a certain regression model (represented by the first subscript letter, with I and T represent crop specific model and the combined model, respectively). A comparison between the first two indictors was to test the stability of a VI for FPAR estimation across different crops. The third indictor reveals the sensitivity of an index to crop types: the smaller the value, the less sensitive the index.

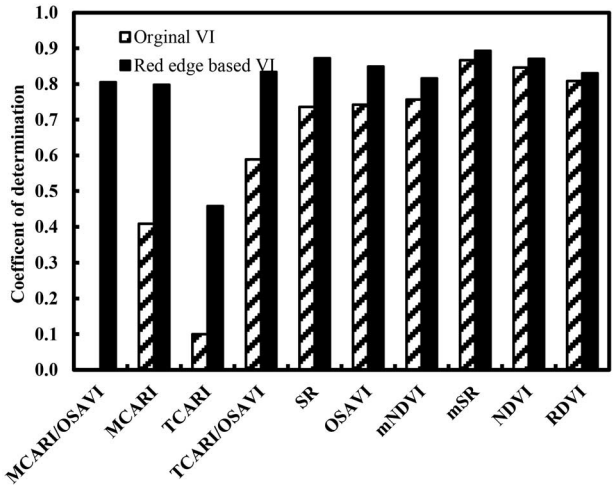

Fig. 4. Comparison between the original and the red-edge-based VIs in correlation with crop FPAR.

Since R^2 could be misleading when the regression model is nonlinear, the noise equivalent FPAR ($NE_{\Delta FPAR}$) [5], [12] using the best-fit equation was thus used to further analyze the stability of the tested VIs for crop FPAR estimation:

$$NE_{\Delta FPAR} = \delta_{\mathrm{VI}}/(\delta \mathrm{VI}/\delta FPAR) \quad (4)$$

where δ_{VI} is the RMSE derived from the best fit function between VI and FPAR, and $\partial \mathrm{VI}/\partial \mathrm{FPAR}$ is the partial derivative of the fit function. A consistent smaller $\mathrm{NE}_{\Delta \mathrm{FPAR}}$ across the whole dynamic range of FPAR represents a better index for crop FPAR estimation [12].

III. Results and Discussions

A. Regression Analysis Between Crop FPAR and the VIs

Results of the initial linear regression analysis between the VIs and the measured crop FPAR for the two crops combined are given in Table II. The R^2 of the indices varied between 0 and 0.89, and the RMSE varied between 0.09 and 0.27. Most of the VIs had a positive correlation with crop FPAR, except for MCARI/OSAVI[705, 750], TCARI/OSAVI, TCARI[705, 750], and TGI. Except for TCARI, TGI, and MCARI/OSAVI ($R^2 \leq 0.10$), the indices were statistically significantly correlated with FPAR ($R^2 > 0.23$, $\mathrm{RMSE} < 0.27$). The mSR2 was the best to correlate with FPAR ($R^2 = 0.89$, $\mathrm{RMSE} = 0.09$), followed by SR_{705}, ND_{705}, MSR, MTCI, OSAVI[705, 750], and NDVI.

VIs developed with particular intention for leaf level chlorophyll content estimation had a relatively weaker correlation with FPAR. This includes the triangular-based indices (e.g.,

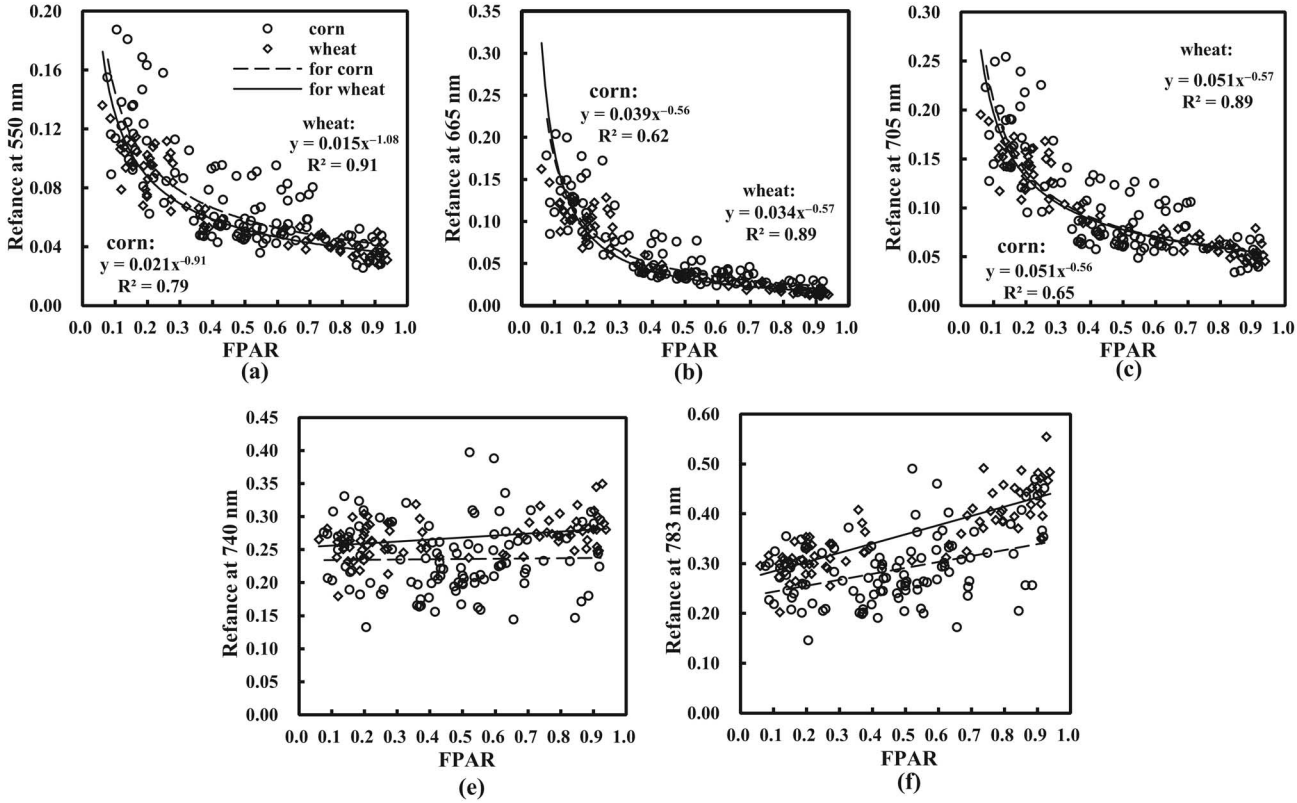

Fig. 5. Relationships between crop FPAR and canopy reflectance at 560, 665, 705, 740, and 783 nm, correspondent to Sentinel-2 Bands 3–7.

TABLE III
RESULTS FROM THE BEST-FIT REGRESSION USING THE SAMPLES FROM CORN OR WHEAT BETWEEN FPAR AND THE VIs

	Corn (n = 104)			Wheat (n = 83)		
Vegetation index	Equation	R^2	RMSE	Equation	R^2	RMSE
mSR2	y = 0.506x+0.037	0.85	0.09	y = 0.539x–0.062	0.95	0.07
SR_{705}	y = 0.526ln(x)–0.0232	0.84	0.09	y = 0.611ln(x)–0.1667	0.95	0.07
ND_{705}	y = –0.594ln(–1.040x+0.924)	0.85	0.09	y = –0.868ln(–1.080x+1.110)	0.95	0.07
mSR	y = 2.632ln(0.101x+1.005)	0.89	0.08	y = 0.991ln(0.294x+0.926)	0.96	0.06
MTCI	y = 0.627ln(0.161x+1.100)	0.82	0.10	y = 0.657ln(0.217x+0.833)	0.95	0.07
OSAVI[705,750]	y = 22.112ln(0.092x+0.996)	0.81	0.10	y = 33.46ln(0.072x+0.990)	0.92	0.09
NDVI	y = –0.459ln(–1.139x+0.878)	0.82	0.08	y = –0.400ln(–1.201x+1.229)	0.97	0.06
TCARI/OSAVI[705,750]	y = 2.695ln(–0.404x+1.405)	0.73	0.14	y = 1.005ln(–1.171x+2.146)	0.94	0.08
GNDVI	y = –0.497ln(–1.570x+1.278)	0.86	0.11	y = –0.49ln(–1.686x+1.491)	0.93	0.08
$RDVI_{705}$	y = –0.999ln(–1.379x+1.055)	0.83	0.12	y = –1.199ln(–1.235x+1.151)	0.92	0.10
$CI_{red\text{-}edge}$[750]	y = 0.529ln(0.637x+1.047)	0.85	0.09	y = 0.554ln(0.542x+0.830)	0.95	0.07

Note: x represents VI and y represents FPAR; R^2 is the coefficient of determination; RMSE is the RMSE of FPAR ($P < 0.05$).

TCARI, MCARI, TCI, and TGI) and their combination with another index (e.g., TCARI/OSAVI) to enhance leaf level chlorophyll content detection while suppressing the variability of canopy LAI [64]. Since LAI is a dominant factor of canopy FPAR, the performance of these indices for FPAR estimation is compromised.

For the indices with an R^2 higher than 0.83 from the linear regression analysis in Table II, a best-fit function was derived using an exponential or a power regression model. The scatterplot between the measured FPAR and these indices are shown in Fig. 3. $RDVI_{705}$ and mSR2 were more linearly correlated with FPAR, whereas the other indices were slightly deviate from a linear correlation.

B. Effects of the Red-Edge Reflectance on Crop FPAR Estimation

To investigate the effects using the red-edge reflectance for FPAR estimation, R^2 of a few conventional indices and that of the revised version incorporating the red-edge reflectance are shown in Fig. 4. Here, incorporating the red-edge reflectance into an index refers to using the red-edge reflectance to replace the reflectance of the band(s) to the shorter (red or red-edge close to red band) or the longer wavelength (near-infrared) directions. It can be observed that incorporating the red-edge reflectance in conventional VIs generally increased the correlation with FPAR. For instance, the R^2 of ND_{705} (0.87)

and mSR2 (0.89) were higher than the corresponding R^2 of NDVI (0.85) and mSR (0.87). More apparently, R^2 of OSAVI (using reflectance at 800 and 670 nm) was 0.74, much lower than that of OSAVI [705, 750] (0.85). Significant improvement in correlation with FPAR was observed for the indices MCARI/OSAVI, MCARI, TCARI, and TCARI/OSAVI, when the red-edge reflectance is used. This possibly was because the red-edge reflectance was more responsive than the red reflectance to variation in LAI [37], [38], [44]; therefore, the indices using the red-edge reflectance was more responsive to FPAR. From Table II and Fig. 4, it was also interesting to observe that $\mathrm{CI_{red\text{-}edge}}$[750] had a stronger correlation with FPAR than $\mathrm{CI_{red\text{-}edge}}$[705]. This possibly was because the red-edge band of Sentinel-2 centered at 740 nm was farther away from the red band than the red-edge band centered at 705 nm, thus was more responsive to FPAR at larger FPAR. Furthermore, SR_{705}, using both of the red-edge bands, had a stronger correlation with FPAR than that using only one of the bands, e.g., $\mathrm{CI_{red\text{-}edge}}$[750]. Our results were in conformity with the study of [44], which showed that $\mathrm{CI_{red\text{-}edge}}$[750] was better than $\mathrm{CI_{red\text{-}edge}}$[705] for canopy chlorophyll content estimation, as crop FPAR had a stronger correlation with canopy chlorophyll content.

C. Effects of Crop Type

Corn and wheat have different canopy structures (i.e., the spatial arrangement and orientation of plant components) and physiological pathways (C3 vs. C4). In general, leaf angle distribution of corn is spherical and of wheat is uniform [21]. The leaf-sun geometry influences PAR interception [21], [65] and canopy reflectance significantly [37], [43]. Fig. 5 shows the scatter-plots between FPAR and the simulated reflectance in the visible, red-edge, and near-infrared regions of the Sentinel-2 bands for the two crops, together with their regression models. The fitted models for the two crops were different for the red and the green reflectance, more apparent for the green reflectance. Regression models for the red-edge reflectance at 705 nm were similar for the two crops, with approximately the same regression coefficients. Fig. 5 also showed that the relationship between the NIR at 783 nm and FPAR was more sensitive to crop types than that of the visible and the 705 nm red-edge bands. The reflectance at 750 nm appears to be relatively independent of FPAR. This indicates that the red-edge reflectance is relatively more independent of crop types than that at the green, red, and the near-infrared bands.

Results of regression analyses between FPAR and VIs for each of the two crops using the best fit model (either linear or nonlinear) are given in Table III. In addition, regression analysis was also performed using samples from both crops combined (results not shown). Relative variation in errors calculated using (3) is shown in Fig. 6. It was observed from Table III that the best regression model for mSR2 was linear for both crops, whereas for other indices was nonlinear. NDVI had the lowest estimation error for each individual crop (0.08 for corn and 0.06 for wheat). This indicates that it is a stable estimator for FPAR for a specific crop. Most VIs had a large relative variation in estimation errors obtained using the crop-specific

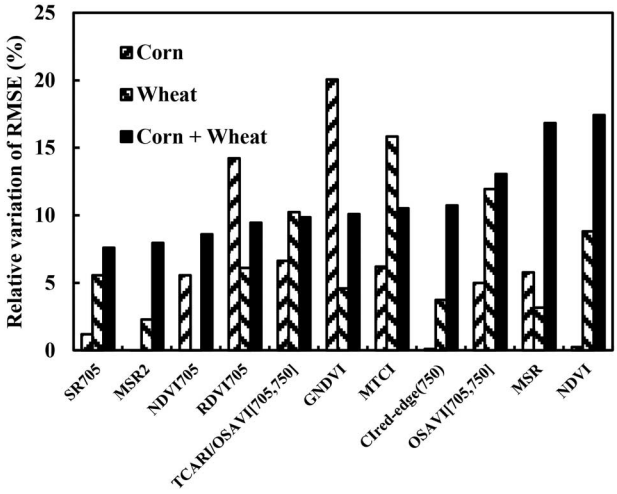

Fig. 6. Relative variation in RMSE for corn, wheat, and the two crops combined; the relative variation of RMSE for a given sample set was calculated as the absolute difference between the estimation error using the crop specific regression models and that using the combined regression model, relative to the RMSE obtained using the combined regression model (3).

regression models and the combined regression model (Fig. 6). For wheat, large variation in error was observed for RDVI_{705}, TCARI/OSAVI[705, 750], and GNDVI, whereas for corn, the large variation in error was observed for MTCI, OSAVI[705, 750], TCARI/OSAVI[705, 750], and NDVI. For both crops, the variation in errors was smallest for SR_{705} and mSR2 and largest for MSR and NDVI. This means that the relationship between NDVI (and MSR) and FPAR is highly dependent on crop type, consistent with the observations in [10], [17] that it is highly affected by leaf orientation. On the contrary, our results showed that the red-edge based VIs, such as SR_{705} and mSR2, were less sensitive to the effect of crop types for crop FPAR estimation. This is because the NIR reflectance is mainly determined by leaf scattering hence is highly dependent on crop types with different leaf angle distribution [12], [37], [43], [50], whereas variation in the red-edge reflectance was impacted by pigment absorption and to a less extent by leaf scattering [36], [37], [43], [50]. This possibly is the reason that the red-edge indices were more consistent estimators of FPAR across different canopy structures [45], [46].

D. Sensitivity Analysis

To further evaluate the performance of the selected VIs, a sensitivity analysis was performed to investigate the variation in $\mathrm{NE}_{\Delta\mathrm{FPAR}}$ as a function of FPAR. The results for the VIs with an R^2 higher than 0.83 (Table II) are shown in Fig. 7. Here, $\mathrm{NE}_{\Delta\mathrm{FPAR}}$ were calculated using the best-fit functions between the indices and the measured FPAR. The results showed that NDVI had the lowest $\mathrm{NE}_{\Delta\mathrm{FPAR}}$ when $\mathrm{FPAR} < 0.5$ and the highest $\mathrm{NE}_{\Delta\mathrm{FPAR}}$ when $\mathrm{FPAR} > 0.65$, due to a comparatively large difference in sensitivity to FPAR between low and high biomass. The $\mathrm{NE}_{\Delta\mathrm{FPAR}}$ of mSR2 and RDVI_{705} was stable across the entire range of FPAR, with a slightly higher noise level for RDVI_{705}. This indicates that mSR2 and RDVI_{705} might be suitable for FPAR estimation at different

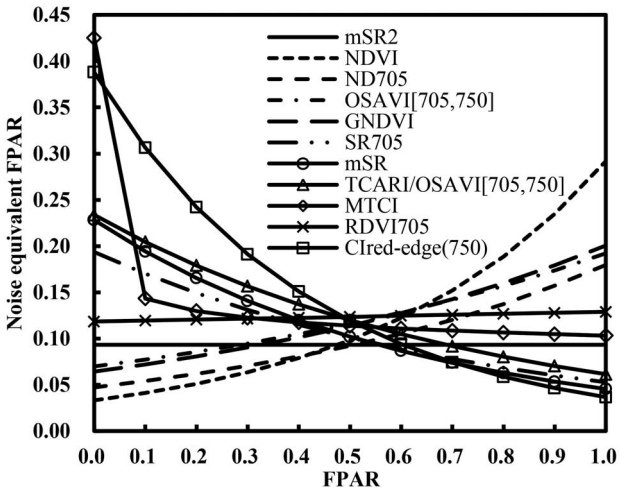

Fig. 7. Noise equivalent of FPAR estimation by VIs.

growth stages using a same regression model. $\mathrm{NE}_{\Delta\mathrm{FPAR}}$ of NDVI, ND_{705}, GNDVI, and OSAVI[705, 750] increased with FPAR, indicating that they were better for FPAR estimation at lower than at higher biomass. This is in conformity to the study by Nguy-Robertson *et al.* [50] that NDVI, GNDVI, and ND_{705} were more accurate for LAI estimation when LAI was below 2. On the contrary, $\mathrm{NE}_{\Delta\mathrm{FPAR}}$ of SR_{705}, mSR, TCARI/OSAVI[705, 750], and $\mathrm{CI}_{\text{red-edge}}$[750] decreased with FPAR, indicating an improved performance for FPAR estimation at higher biomass using these indices. Future study could probably attempt the combination of the above two types of indices, e.g., NDVI and mSR, for an improved estimation of FPAR at both low and high biomass ranges. An improved FPAR estimation model could probably benefit from the advantages of these two types of indices.

IV. Conclusion

The performance of chlorophyll-related VIs was assessed for fractional absorbed photosynthetically active radiation (FPAR) estimation over wheat and corn canopies. Indices developed for leaf level chlorophyll content estimation were observed to have inferior performance for canopy FPAR estimation, whereas indices that captured canopy chlorophyll content and LAI were found to have a much stronger capability in FPAR estimation. This emphasized the importance that VIs effective for FPAR estimation should be sensitive to both LAI and chlorophyll content. Modification of conventional VIs that rely on the contrast between the visible and NIR by incorporating the red-edge reflectance was found to improve their capability for FPAR estimation. The modification is mostly made by replacing the reflectance in the near-infrared or the red bands (or both) with reflectance in the red-edge region. The Modified Simple Ratio Index (mSR2), which is based on the two red-edge reflectance of the Sentinel-2 bands (Bands 5 and 6), had the strongest linear correlation with FPAR of the two crops studied, as well as a consistent lower level of estimation noise across the entire variation range of FPAR. The red-edge indices, such as the mSR2 and SR_{705}, were relatively resistant to the impact from canopy structure.

It is worth noting that this study was based on the simulated Sentinel-2 reflectance using ground-measured canopy reflectance. With the red-edge bands implemented in the Sentinel-2 sensor, higher accuracy FPAR products could be anticipated. However, impacts from other factors, such as the illumination and observation geometry, leaf and soil optical properties, and atmospheric perturbations were not considered in this study. Further studies are necessary to investigate the uncertainty induced by these interference factors for FPAR estimation using data for different crops and at different agricultural environment.

Acknowledgment

The authors would like to thank Dr. M. Zhang and Mr. X. You for their help in collecting field measurements and also the three anonymous reviews for their valuable comments and suggestions.

References

[1] A. McCallum *et al.*, "Comparison of four global FAPAR datasets over Northern Eurasia for the year 2000," *Remote Sens. Environ.*, vol. 114, pp. 941–949, May 2010.

[2] B. Martínez, F. Camacho, A. Verger, F. J. García-Haro, and M. A. Gilabert, "Intercomparison and quality assessment of MERIS, MODIS and SEVIRI FAPAR products over the Iberian Peninsula," *Int. J. Appl. Earth Observ. Geoinf.*, vol. 21, pp. 463–476, 2013.

[3] M. Claverie *et al.*, "Maize and sunflower biomass estimation in southwest France using high spatial and temporal resolution remote sensing data," *Remote Sens. Environ.*, vol. 124, pp. 844–857, Sep. 2012.

[4] Y.-B. Cheng, Q. Zhang, A. I. Lyapustin, Y. Wang, and E. M. Middleton, "Impacts of light use efficiency and fPAR parameterization on gross primary production modeling," *Agric. Forest Meteorol.*, vol. 189, pp. 187–197, 2014.

[5] A. A. Gitelson, Y. Peng, and K. F. Huemmrich, "Relationship between fraction of radiation absorbed by photosynthesizing maize and soybean canopies and NDVI from remotely sensed data taken at close range and from MODIS 250 m resolution data," *Remote Sens. Environ.*, vol. 147, pp. 108–120, 2014.

[6] B. Ogutu, J. Dash, and T. P. Dawson, "Evaluation of the influence of two operational fraction of absorbed photosynthetically active radiation (FAPAR) products on terrestrial ecosystem productivity modelling," *Int. J. Remote Sens.*, vol. 35, pp. 321–340, 2014.

[7] N. Gobron and M. Verstraete, "Assessment of the status of the development of the standards for the terrestrial essential climate variables: T10 FAPAR," FAO, Rome, Tech. Rep. GTOS-65, Nov. 2009.

[8] Q. Zhang, E. M. Middleton, Y.-B. Cheng, and D. R. Landis, "Variations of foliage chlorophyll fAPAR and foliage non-chlorophyll fAPAR (fAPAR, fAPAR) at the Harvard forest," *IEEE J. Sel. Topics Appl. Earth Observ. Remote Sens.*, vol. 6, no. 5, pp. 2254–2264, Oct. 2013.

[9] A. Verger, F. Baret, and F. Camacho, "Optimal modalities for radiative transfer-neural network estimation of canopy biophysical characteristics: Evaluation over an agricultural area with CHRIS/PROBA observations," *Remote Sens. Environ.*, vol. 115, pp. 415–426, 2011.

[10] J.-L. Roujean and F.-M. Breon, "Estimating PAR absorbed by vegetation from bidirectional reflectance measurements," *Remote Sens. Environ.*, vol. 51, pp. 375–384, 1995.

[11] N. Gobron *et al.*, "Monitoring FAPAR over land surfaces with remote sensing data," in *Remote Sensing for Agriculture, Ecosystems, and Hydrology V*, vol. 5232, M. Owe, G. Durso, J. F. Moreno, and A. Calera, Eds. Bellingham, WA, USA: SPIE-Int. Soc. Optical Eng., 2004, pp. 237–244.

[12] A. Vina and A. A. Gitelson, "New developments in the remote estimation of the fraction of absorbed photosynthetically active radiation in crops," *Geophys. Res. Lett.*, vol. 32, p. L17403, Sep. 2005.

[13] C. Bacour, F. Baret, D. Béal, M. Weiss, and K. Pavageau, "Neural network estimation of LAI, fAPAR, fCover and $\mathrm{LAI} \times \mathrm{Cab}$, from top of canopy MERIS reflectance data: Principles and validation," *Remote Sens. Environ.*, vol. 105, pp. 313–325, 2006.

[14] F. Baret *et al.*, "LAI, fAPAR and fCover CYCLOPES global products derived from VEGETATION: Part 1: Principles of the algorithm," *Remote Sens. Environ.*, vol. 110, pp. 275–286, 2007.

[15] Q. Zhang *et al.*, "Can a satellite-derived estimate of the fraction of PAR absorbed by chlorophyll (FAPARchl) improve predictions of light-use efficiency and ecosystem photosynthesis for a boreal aspen forest?," *Remote Sens. Environ.*, vol. 113, pp. 880–888, 2009.

[16] K. F. Huemmrich and S. N. Goward, "Vegetation canopy PAR absorptance and NDVI: An assessment for ten tree species with the SAIL model," *Remote Sens. Environ.*, vol. 61, pp. 254–269, 1997.

[17] R. B. Myneni and D. L. Williams, "On the relationship between FAPAR and NDVI," *Remote Sens. Environ.*, vol. 49, pp. 200–211, 1994.

[18] T. Dong, J. Meng, and B. Wu, "Overview on methods of deriving fraction of absorbed photosynthetically active radiation (FPAR) using remote sensing," *Acta Ecol. Sinica*, vol. 32, pp. 7190–7201, 2012.

[19] Y. Knyazikhin *et al.*, "Estimation of vegetation canopy leaf area index and fraction of absorbed photosynthetically active radiation from atmosphere-corrected MISR data," *J. Geophys. Res. Atmos.*, vol. 103, pp. 32239–32256, Dec. 1998.

[20] R. B. Myneni *et al.*, "Global products of vegetation leaf area and fraction absorbed PAR from year one of MODIS data," *Remote Sens. Environ.*, vol. 83, pp. 214–231, 2002.

[21] A. Viña, A. A. Gitelson, A. L. Nguy-Robertson, and Y. Peng, "Comparison of different vegetation indices for the remote assessment of green leaf area index of crops," *Remote Sens. Environ.*, vol. 115, pp. 3468–3478, 2011.

[22] J. N. Epiphanio and A. R. Huete, "Dependence of NDVI and SAVI on sun/sensor geometry and its effect on fAPAR relationships in Alfalfa," *Remote Sens. Environ.*, vol. 51, pp. 351–360, Mar. 1995.

[23] B. Pinty, T. Lavergne, J. L. Widlowski, N. Gobron, and M. M. Verstraete, "On the need to observe vegetation canopies in the near-infrared to estimate visible light absorption," *Remote Sens. Environ.*, vol. 113, pp. 10–23, Jan. 2009.

[24] Q. Zhang *et al.*, "Estimation of crop gross primary production (GPP): II. Do scaled MODIS vegetation indices improve performance?," *Agric. Forest Meteorol.*, vol. 200, pp. 1–8, Jan. 2015.

[25] J. Liu *et al.*, "Estimating crop stresses, aboveground dry biomass and yield of corn using multi-temporal optical data combined with a radiation use efficiency model," *Remote Sens. Environ.*, vol. 114, pp. 1167–1177, 2010.

[26] G. P. Asner, C. A. Wessman, and S. Archer, "Scale dependence of absorption of photosynthetically active radiation in terrestrial ecosystems," *Ecol. Appl.*, vol. 8, pp. 1003–1021, 1998.

[27] A. A. Gitelson and J. A. Gamon, "The need for a common basis for defining light-use efficiency: Implications for productivity estimation," *Remote Sens. Environ.*, vol. 156, pp. 196–201, Jan. 2015.

[28] F. G. Hall, K. F. Huemmrich, S. J. Goetz, P. J. Sellers, and J. E. Nickeson, "Satellite remote sensing of surface energy balance: Success, failures, and unresolved issues in FIFE," *J. Geophys. Res.*, vol. 97, pp. 19061–19089, 1992.

[29] Q. Zhang *et al.*, "Estimating light absorption by chlorophyll, leaf and canopy in a deciduous broadleaf forest using MODIS data and a radiative transfer model," *Remote Sens. Environ.*, vol. 99, pp. 357–371, 2005.

[30] A. Harris and J. Dash, "A new approach for estimating northern peatland gross primary productivity using a satellite-sensor-derived chlorophyll index," *J. Geophys. Res. Biogeosci. (2005–2012)*, vol. 116, p. G04002, 2011.

[31] Y. Peng and A. A. Gitelson, "Remote estimation of gross primary productivity in soybean and maize based on total crop chlorophyll content," *Remote Sens. Environ.*, vol. 117, pp. 440–448, 2012.

[32] Y. Peng, A. A. Gitelson, G. Keydan, D. C. Rundquist, and W. Moses, "Remote estimation of gross primary production in maize and support for a new paradigm based on total crop chlorophyll content," *Remote Sens. Environ.*, vol. 115, pp. 978–989, Apr. 2011.

[33] T. Dong *et al.*, "Sensitivity analysis of retrieving fraction of absorbed photosynthetically active radiation (FPAR) using remote sensing data," *Acta Ecol. Sinica*, to be published.

[34] B. O. Ogutu and J. Dash, "An algorithm to derive the fraction of photosynthetically active radiation absorbed by photosynthetic elements of the canopy (FAPARps) from eddy covariance flux tower data," *New Phytol.*, vol. 197, pp. 511–523, Jan. 2013.

[35] A. A. Gitelson, Y. Peng, T. J. Arkebauer, and J. Schepers, "Relationships between gross primary production, green LAI, and canopy chlorophyll content in maize: Implications for remote sensing of primary production," *Remote Sens. Environ.*, vol. 144, pp. 65–72, Mar. 2014.

[36] J. Delegido, J. Verrelst, L. Alonso, and J. Moreno, "Evaluation of Sentinel-2 red-edge bands for empirical estimation of green LAI and chlorophyll content," *Sensors*, vol. 11, pp. 7063–7081, 2011.

[37] C. Wu, Z. Niu, Q. Tang, and W. Huang, "Estimating chlorophyll content from hyperspectral vegetation indices: Modeling and validation," *Agric. Forest Meteorol.*, vol. 148, pp. 1230–1241, 2008.

[38] D. Haboudane, N. Tremblay, J. R. Miller, and P. Vigneault, "Remote estimation of crop chlorophyll content using spectral indices derived from hyperspectral data," *IEEE Trans. Geosci. Remote Sens.*, vol. 46, no. 2, pp. 423–437, Feb. 2008.

[39] A. A. Gitelson, Y. Gritz, and M. N. Merzlyak, "Relationships between leaf chlorophyll content and spectral reflectance and algorithms for non-destructive chlorophyll assessment in higher plant leaves," *J. Plant Physiol.*, vol. 160, pp. 271–282, 2003.

[40] C. S. T. Daughtry, C. L. Walthall, M. S. Kim, E. B. de Colstoun, and J. E. McMurtrey, III, "Estimating corn leaf chlorophyll concentration from leaf and canopy reflectance," *Remote Sens. Environ.*, vol. 74, pp. 229–239, Nov. 2000.

[41] E. R. Hunt, Jr. *et al.*, "A visible band index for remote sensing leaf chlorophyll content at the canopy scale," *Int. J. Appl. Earth Observ. Geoinf.*, vol. 21, pp. 103–112, Apr. 2013.

[42] P. J. Zarco-Tejada, J. Miller, A. Morales, A. Berjón, and J. Agüera, "Hyperspectral indices and model simulation for chlorophyll estimation in open-canopy tree crops," *Remote Sens. Environ.*, vol. 90, pp. 463–476, 2004.

[43] A. L. Nguy-Robertson *et al.*, "Estimating green LAI in four crops: Potential of determining optimal spectral bands for a universal algorithm," *Agric. Forest Meteorol.*, vol. 192–193, pp. 140–148, Jul. 2014.

[44] M. Schlemmer *et al.*, "Remote estimation of nitrogen and chlorophyll contents in maize at leaf and canopy levels," *Int. J. Appl. Earth Observ. Geoinf.*, vol. 25, pp. 47–54, 2013.

[45] A. A. Gitelson, A. Vina, V. Ciganda, D. C. Rundquist, and T. J. Arkebauer, "Remote estimation of canopy chlorophyll content in crops," *Geophys. Res. Lett.*, vol. 32, p. L08403, 2005.

[46] A. A. Gitelson, G. P. Keydan, and M. N. Merzlyak, "Three-band model for noninvasive estimation of chlorophyll, carotenoids, and anthocyanin contents in higher plant leaves," *Geophys. Res. Lett.*, vol. 33, p. L11402, 2006.

[47] J. Dash and P. Curran, "The MERIS terrestrial chlorophyll index," *Int. J. Remote Sens.*, vol. 25, pp. 5403–5413, 2004.

[48] J. Dash *et al.*, "Validating the MERIS terrestrial chlorophyll index (MTCI) with ground chlorophyll content data at MERIS spatial resolution," *Int. J. Remote Sens.*, vol. 31, pp. 5513–5532, 2010.

[49] C. Tan *et al.*, "Using hyperspectral vegetation indices to estimate the fraction of photosynthetically active radiation absorbed by corn canopies," *Int. J. Remote Sens.*, vol. 34, pp. 8789–8802, Dec. 2013.

[50] A. Nguy-Robertson *et al.*, "Green leaf area index estimation in maize and soybean: Combining vegetation indices to achieve maximal sensitivity," *Agron. J.*, vol. 104, pp. 1336–1347, 2012.

[51] F. Camacho, J. Cernicharo, R. Lacaze, F. Baret, and M. Weiss, "GEOV1: LAI, FAPAR essential climate variables and FCOVER global time series capitalizing over existing products. Part 2: Validation and intercomparison with reference products," *Remote Sens. Environ.*, vol. 137, pp. 310–329, Oct. 2013.

[52] J. Chen *et al.*, "A simple method for reconstructing a high-quality NDVI time-series data set based on the Savitzky–Golay filter," *Remote Sens. Environ.*, vol. 91, pp. 332–344, Jun. 30, 2004.

[53] K. Segl, R. Richter, T. Küster, and H. Kaufmann, "End-to-end sensor simulation for spectral band selection and optimization with application to the Sentinel-2 mission," *Appl. Opt.*, vol. 51, pp. 439–449, 2012.

[54] J. W. Rouse, R. H. Haas, J. A. Schell, and D. W. Deering, "Monitoring vegetation systems in the Great Plains with ERTS," in *Proc. 3rd ERTS Symp.*, Washington, DC, USA, 1973, pp. 309–317.

[55] A. Gitelson and M. N. Merzlyak, "Quantitative estimation of chlorophyll-a using reflectance spectra: Experiments with autumn chestnut and maple leaves," *J. Photochem. Photobiol. B: Biol.*, vol. 22, pp. 247–252, Mar. 1994.

[56] D. A. Sims and J. A. Gamon, "Relationships between leaf pigment content and spectral reflectance across a wide range of species, leaf structures and developmental stages," *Remote Sens. Environ.*, vol. 81, pp. 337–354, Aug. 2002.

[57] Q. Cao *et al.*, "Non-destructive estimation of rice plant nitrogen status with crop circle multispectral active canopy sensor," *Field Crops Res.*, vol. 154, pp. 133–144, Dec. 2013.

[58] A. A. Gitelson, Y. J. Kaufman, and M. N. Merzlyak, "Use of a green channel in remote sensing of global vegetation from EOS-MODIS," *Remote Sens. Environ.*, vol. 58, pp. 289–298, 1996.

[59] G. Rondeaux, M. Steven, and F. Baret, "Optimization of soil-adjusted vegetation indices," *Remote Sens. Environ.*, vol. 55, pp. 95–107, 1996.
[60] J. M. Chen, "Evaluation of vegetation indices and a modified simple ratio for boreal applications," *Can. J. Remote Sens.*, vol. 22, pp. 229–242, 1996.
[61] J. M. Chen, "Canopy architecture and remote sensing of the fraction of photosynthetically active radiation absorbed by boreal conifer forests," *IEEE Trans. Geosci. Remote Sens.*, vol. 34, no. 6, pp. 1353–1368, Nov. 1996.
[62] N. H. Broge and E. Leblanc, "Comparing prediction power and stability of broadband and hyperspectral vegetation indices for estimation of green leaf area index and canopy chlorophyll density," *Remote Sens. Environ.*, vol. 76, pp. 156–172, May 2001.
[63] E. R. Hunt, C. S. T. Daughtry, J. U. H. Eitel, and D. S. Long, "Remote sensing leaf chlorophyll content using a visible band index," *Agron. J.*, vol. 103, pp. 1090–1099, Jul. 2011.
[64] D. Haboudane, J. R. Miller, N. Tremblay, P. J. Zarco-Tejada, and L. Dextraze, "Integrated narrow-band vegetation indices for prediction of crop chlorophyll content for application to precision agriculture," *Remote Sens. Environ.*, vol. 81, pp. 416–426, Aug. 2002.
[65] J. Bendix *et al.*, "Model parameterization to simulate and compare the PAR absorption potential of two competing plant species," *Int. J. Biometeorol.*, vol. 54, pp. 283–295, 2010.

Taifeng Dong received the Bachelor's degree in geographic information system from Central South University (CSU), Changsha, Hunan, China, and the Ph.D. degree in cartography and remote sensing from the Institute of Remote Sensing and Digital Earth (RADI), Chinese Academy of Sciences (CAS), Beijing, China, in 2008 and 2013, respectively.

He is currently a Postdoc Fellow with the Science and Technology Branch of Agriculture and Agri-Food Canada (AAFC), Ottawa, Canada. His research interests include biophysical variable estimation and crop growth modeling using remote sensing.

Jihua Meng received the M.S. degree in remote sensing application in mineral exploration from Xinjiang University, Xinjiang, China, and the Ph.D. degree in cartography and remote sensing from the Institute of Remote Sensing and Digital Earth (RADI), Chinese Academy of Sciences (CAS), Beijing, China, in 2003 and 2006, respectively.

Currently, he is a Professor with the RADI, CAS. He has authored more than 80 papers. His research interests include remote sensing application in agriculture.

Jiali Shang (M'12) received the B.Sc. degree in geography from Beijing Normal University, Beijing, China, the M.A. degree from the University of Windsor, Windsor, ON, Canada, and the Ph.D. degree in remote sensing from the University of Waterloo, Waterloo, ON, Canada, in 1984, 1996, and 2005, respectively.

Currently, she is a Research Scientist with the Science and Technology Branch of Agriculture and Agri-Food Canada (AAFC), Ottawa, ON, Canada. She specializes in method development of optical and radar integration for agriculture applications.

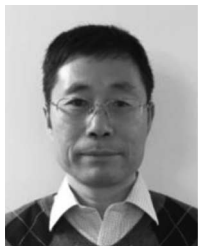

Jiangui Liu received the Bachelor's degree in electronics engineering from Tsinghua University, Beijing, China, and the Ph.D. degree in cartography and remote sensing from the Chinese Academy of Sciences (CAS), Beijing, China, in 1990 and 1999.

Currently, he is a Physical Scientist with the Science and Technology Branch, Agriculture and Agri-Food Canada (AAFC). His research interests include using remote sensing for crop and soil biophysical parameters estimation, crop productivity, and agri-environmental sustainability assessment.

Bingfang Wu received the M.S. degree in water resources and system analysis from Tianjin University, Tianjin, China, and the Ph.D. degree in environmental planning and management from Tsinghua University, Tsinghua, China, in 1985 and 1989, respectively.

Currently, he is a Professor with the Institute of Remote Sensing and Digital Earth (RADI), Chinese Academy of Sciences (CAS), Beijing, China. He is the Co-Chair of the GEO/GEOSS Global Agricultural Monitoring Task. He has authored more than 250 papers and has written one book. His research interests include crop monitoring with remote sensing, water resources monitoring, and regional/global eco-environment evaluation.